WORLD CONFERENCE ON TIMBER ENGINEERING 2025
BRISBANE, AUSTRALIA
Advancing Timber for the Future Built Environment

SEISMIC COLLAPSE ASSESSMENT OF TIMBER BRACED FRAMES WITH FRICTION JOINTS USING FEMA P695 METHODOLOGY

Mohammadmahdi Gholami[1], Christian Viau[2], Ghasan Doudak[3]

ABSTRACT: Little research has been conducted on the behaviour of timber seismic load resisting systems using friction joints (FJs), particularly those involving timber braced frames (TBFs). This paper proposes seismic design parameters for timber braced frames with friction joints (TBFFJs) and evaluates their performance using the FEMA P695 methodology. A hysteresis model is developed and implemented in OpenSees and validated against existing experimental results. A total of three multi-storey (3-, 6-, and 12-storey) structures with TBFFJs were analyzed using the proposed model to validate the design methodology. Static pushover and incremental dynamic analyses using 44 ground motions were conducted and adjusted collapse margin ratio were compared with allowable limits provided in FEMA P695. Response modification factors are determined and proposed based on the results of these analyses.

KEYWORDS: timber braced frames, friction joints, FEMA P695, seismic assessment, ductility

1 - INTRODUCTION

Timber braced frames (TBFs) have been used in construction as a lateral load resisting system (LLRS), since they possess high strength and stiffness but tend to have limited or moderate ductility and displacement capacity when traditional dowel-type connectors are used. The performance of the connections is paramount since the system primarily relies on the brace connections for energy dissipation. The National Building Code of Canada (NBCC) [1] currently categorizes TBFs as moderately ductile or limited ductility LLRS, however, associated design provisions and detailing for TBF systems and connections are not fully developed in the Canadian wood design standard [2] to achieve the performance criteria outlined in the NBCC [1].

Design procedures for TBFs have been proposed emphasizing the need to ensure the presence of ductile connections in the brace connections while the rest of the frame is designed to remain elastic [3,4]. Baird et al. [5] investigated bolted connections to be used in TBFs with internal steel knife plates detailed to ensure yielding occurs in one or both ends of the brace. The authors highlighted the importance of fastener dimensions and connection geometry and noted that increasing the fastener spacing significantly improved the ductility of the connection [5–7]. The studies also emphasized the importance of bolt slenderness on the behaviour of the connections and the system accordingly [6,7]. The main drawback of the system is its significant dependence on the performance of fasteners, which may not always develop effective hysteretic energy dissipation, depending on the design detailing of the connection, such as spacing and slenderness of the fasteners, and whether self-tapping screws (STS) are used for reinforcement [8].

Self-centering friction joints [9], buckling-resistant braces (BRBs) [10], and friction dampers [11] have been utilized in TBFs subjected to seismic demands. Fitzgerald et al. [12] studied the effects of using friction joints (FJs) as hold-downs in cross-laminated timber (CLT) shear walls under cyclic loading, along with STS to prevent any initial slip. Their results demonstrated that the use of FJs can lead to a stable rectangular hysteretic response. Tjahyadi [13] investigated friction dampers in TBFs, with the aim to prevent pinching effect due to oversized bolt-holes. To reach this goal, a friction coefficient between wood and steel side plate was considered in order to calculate the capping force on each bolt in order to prevent wood-to-steel connection from slipping. However, the results showed

[1] Mohammadmahdi Gholami, PhD Candidate, Carleton University, Ottawa, Canada, mohammadmahdigholami@cmail.carleton.ca

[2] Christian Viau, Assistant Professor, Carleton University, Ottawa, Canada, christian.viau@carleton.ca

[3] Ghasan Doudak, Professor, University of Ottawa, Ottawa, Canada, gdoudak@uottawa.ca

https://doi.org/10.52202/080513-0546

that preventing slack in wood-steel connection is not achievable in most cases.

The current study introduces seismic design coefficients and factors timber braced frames with friction joints (TBFFJs) in order to dissipate energy in the FJ while capacity-protecting other connections and structural elements against unwanted brittle failures. A numerical model is proposed and validated against published experimental test results. Three archetypes were designed and analyzed using the FEMA P695 [14] procedure in order to assess the seismic performance of TBFFJs and provide design recommendations for ductility and overstrength factors (OSF) for highly ductile TBFFJs. The seismic performance and design coefficients and factors were established through quantifying collapse margin ratios (CMR) to ensure acceptable probabilities of collapse under maximum considered earthquake (MCE).

2 - MODELLING APPROACH AND VALIDATION

For the purpose of this study, a symmetric FJ, consisting of a slotted plate, two shims, two cap plates, and high-strength bolts, is considered, as shown in Fig. 1 (a). Brass shims were chosen, as the material provides consistent energy dissipation throughout multiple cyclic loading, with minimal wear when in contact with steel [15–18]. The FJ slip force, F_S, can be determined using (1) [19].

$$F_S = n_s n_b \mu_k N \quad (1)$$

where n_s is the number of slip planes, four per FJ; n_b is the number of clamping bolts, two per FJ; μ_k is the dynamic coefficient of friction, assumed 0.32 [19]; and N is the clamping force per bolt. All steel components in the FJs were designed in accordance with CSA S16 [20].

As discussed, FJs are assumed to dissipate all the energy during seismic events, while the rest of the frame elements and connections remain elastic. It should be noted that the initial stiffness of TBFFJs depends on the axial stiffness of the braces, timber connections, and the components forming the FJs. To capture these behaviours, a two springs-in-series system, where one spring represents the wood-to-steel connections and the second spring represents the FJs (see Fig. 1 (b)), was used alongside a truss element representing the timber brace. For the first spring, representing the wood-to-steel connection, Eurocode 5 [21] provision was used to approximate the stiffness of the dowelled connection, as outlined in (2).

$$K_{ser} = {\rho_m^{1.5} d}/{23} \quad (2)$$

Where ρ_m is the mean density of the timber element at 12% moisture content in ${kg}/{m^3}$, and d is fastener diameter in mm. As noted in Eurocode 5, the abovementioned stiffness should be multiplied by 2.0 for steel-to-timber connections.

The second spring, representing the FJs, was idealized as a combination of springs in parallel and series based on the individual components of the FJ. Cap plates and brass shims are idealized as two sets of springs-in-series acting in parallel. Finally, the spring system representing the cap plates and brass shims is connected in series with a spring representing the stiffness of the slotted plate. The complete system of springs effectively captures the axial stiffness of the FJs (see Fig. 1 (c)).

A hysteric model, capable of taking into account the axial stiffness of the FJ, timber element, boundary connections, as well as the behaviour of the slip surface interface, was developed based on the introduced spring system (see Fig. 1(d)). OpenSees [21] was used to conduct static pushover and incremental dynamic analysis (IDA) due to its computational efficiency, ease of implementation of user material models, and versatility in element types. Published component-level experimental test results [12] were used to validate the proposed hysteretic model. Although STS were used to prevent the initial slack in the experimental study, joint slip between the brass shims and the cap plates prior to contact with the clamping bolts (i.e., chipping point) was still observed in the hysteric curve resulting in a chipping effect in the behaviour of FJ in compression zone (see Fig. 2), defined by a sudden jump in connection force. A hysteresis model was developed based on the existing experimental results and used with a zero-length element to capture the chipping effect. This chipping approximately occurs when compression force reaches 90 % of the slip force according to experimental results [12]. Elastic material properties were assigned to the zero-length element, simulating the wood-to-steel connection behaviour. The hysteric behaviour predicted by the numerical model is shown in Fig. 2, demonstrating good agreement with experimental test results [12].

https://doi.org/10.52202/080513-0546

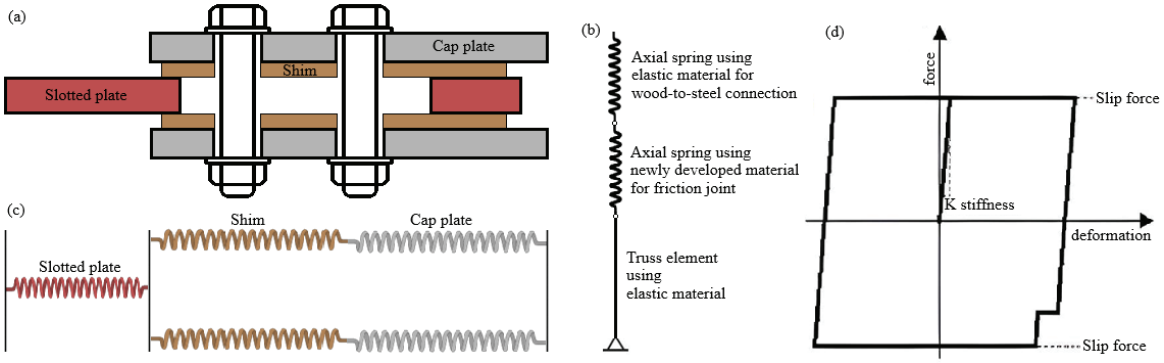

Figure 1. (a) symmetric FJ; (b) analytical series springs model considered for TBFFJ; (c) analytical spring system model considered for FJ; (d) force-deformation relationship assigned to the FJ spring.

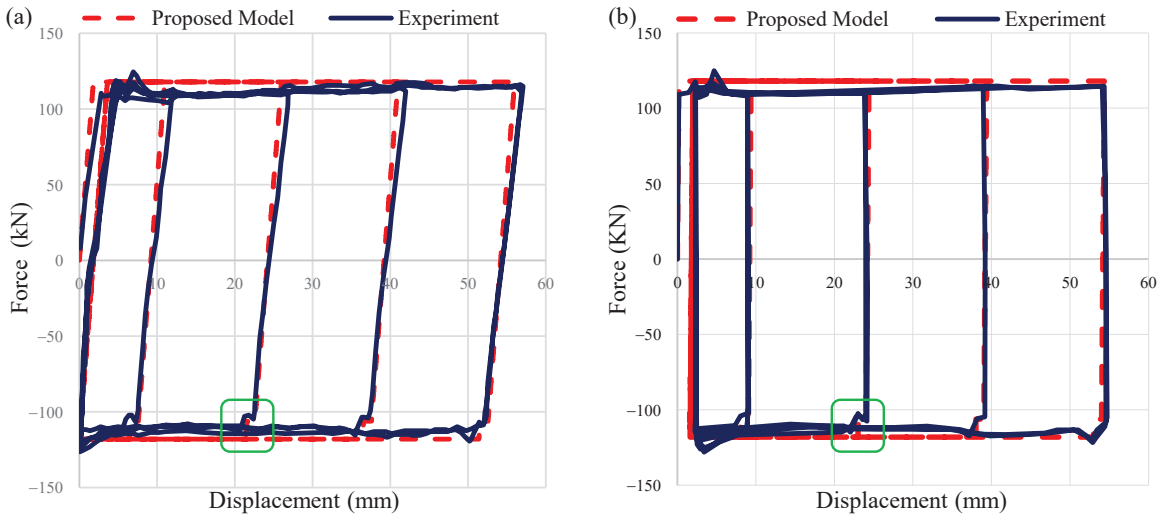

Figure 2. Model verification; (a) hysteresis plots for the displacement of the FJ; (b) and the system deformation with bolt hole slack removed [12]. Chipping points (boxed) observed in the compression zone due to initial slip between the shims and the cap plates prior to contact with the clamping bolts.

3 - DESIGN PROCEDURE

The archetypes studied in this paper consisted of three multi-storey (3-, 6-, and 12-storey) structures, each equipped with TBFFJ as their LLRS. The archetypes are located in D_{max} seismic zone according to FEMA P695, defined as a far-field site with the highest seismicity. All archetypes consisted of 15 m x 15 m symmetric floor plan in which four TBFFJs are designed to resist applied lateral loads in each direction on each floor (see Fig. 3). Response modification coefficient (RMC), R, of 5.0 and an OSF, Ω, of 1.23 were used to design the initial archetypes. These factors obtained after conducting FEMA P695 [14] procedure on the seismic factors for moderately ductile TBFs obtained through the NBCC [1]. The wood elements were designed in accordance with CSA O86-24 [2] while the gravity loads considered for the archetypes were obtained from the estimated element self-weight as well as loading outlined in the NBCC [1]. The storey lateral loads are assumed to be resisted by the TBFFJs only. Within the TBFFJs, the elements (beams, columns, connections) were designed as capacity-protected elements against the forces induced in them when the FJs reach the 95th percentile slip force. This can be achieved using an OSF of 1.38 applied to the seismic loads [19]. In other words, the OSF of 1.7, derived from the multiplication of the two aforementioned factors, is applied to ensure that the non-dissipative elements remain elastic. All timber connections are designed such that the lowest resistance related to a brittle failure mode is at least 60% higher than the governing ductile failure mode to ensure ductile failure modes occur first, to optimize energy dissipation [22].

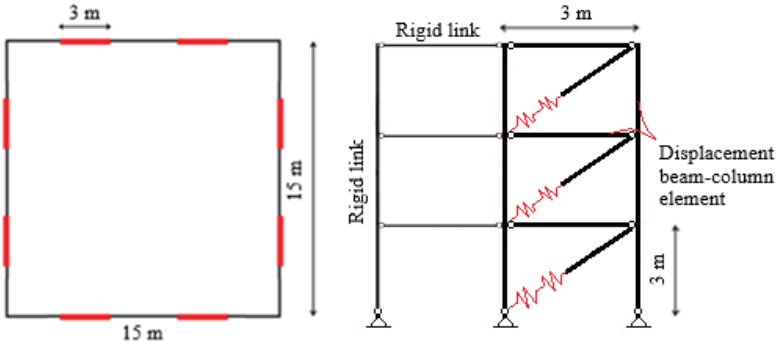

Figure 3. Geometry of buildings plan and TBFFJ system.

4 - ANALYSIS OF THE TBFFJ ARCHETYPES

4.1 STATIC PUSHOVER ANALYSIS AND INCREMENTAL DYNAMIC ANALYSIS

Nonlinear pushover analysis was performed on all TBFFJ archetypes using the proposed developed hysteresis model to extract system OSFs and period-based ductility factors. The descending branch in the secondary slope (see Fig. 4) is due to the P-delta effects, which has been observed in prior studies and do not coincide with instances of structural instabilities [23]. These system over-strength and period-based ductility factors are calculated using (3) and (4):

$$\Omega = \frac{V_{max}}{V_d} \quad (3)$$

$$\mu = \frac{\Delta_u}{\Delta_y} \quad (4)$$

where V_{max} is the maximum base shear obtained from nonlinear pushover analysis; V_d is the design base shear; Δ_u is the ultimate roof displacement; and Δ_y is the yield roof displacement. Fig. 4 includes the nonlinear pushover curves for all archetypes. Considering the second order effect, only the 12-storey building showed a 20% strength loss with regard to the maximum strength before reaching 5% drift, twice that permitted in the NBCC [1].

Incremental dynamic analysis (IDA) [24] was conducted on all archetypes using 44 ground motion records suggested by FEMA P695 guidelines [14]. The 5% damped spectral acceleration at each building's fundamental period of vibration, $S_a(T_1, 5\%)$ was selected as the intensity measure (IM) and the maximum interstorey drift as engineering demand parameter (EDP). This method involves incrementally scaling the intensity of ground motion records to evaluate the structural response at varying levels of seismic intensity. This scaling continues until a predefined EDP or an 80% drop in the slop of IDA curves. Fig. 5 presents and summarizes the IDA results.

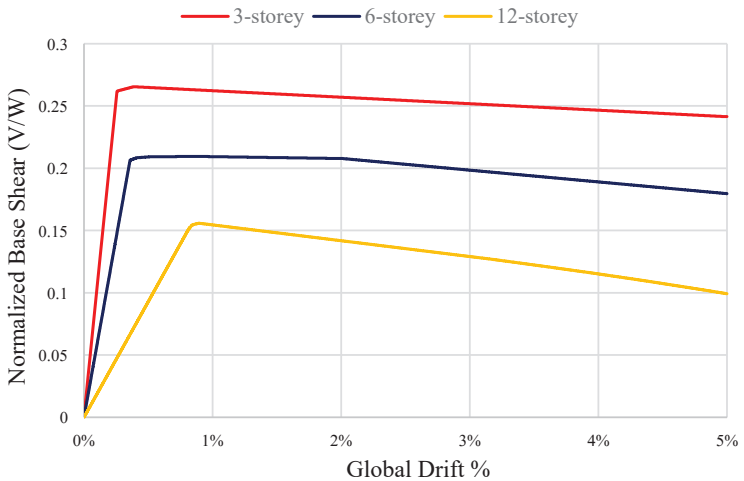

Figure 4. Monotonic pushover analysis results.

https://doi.org/10.52202/080513-0546

4.2 PROBABILISTIC COLLAPSE ASSESSMENT

Collapse fragility curves are often used to determine the probability of collapse of archetypes as a function of the chosen IM. These curves are presented in Fig. 5 for all archetypes. The median collapse capacity (MCC), defined as the IM associated with 50% probability of collapse across all ground motions considered for that archetype and the CMR, are summarized in Table 1. According to FEMA P695 [14], the CMR should be modified to capture the effects of spectral shape on the seismic performance of a structure. This can be achieved by multiplying the CMR with the spectral shape factor (SSF), which can be obtained based on the fundamental period, the period-based ductility, and the seismic design category [14], which is assumed to be D_{max} in this study.

For performance evaluation purposes, and to ensure a consistent level of reliability in accordance with the FEMA P695 procedure, it is essential to quantify uncertainties associated with record-to-record variability (β_{RTR}), design requirements (β_{DR}) availability, quality of test data chosen for verification of numerical model (β_{TD}), and the accuracy and robustness of the modelling methodologies (β_{MDL}). These uncertainties are incorporated together in order to adjust the resulting CMR for the purpose of obtaining appropriate R and μ_T.

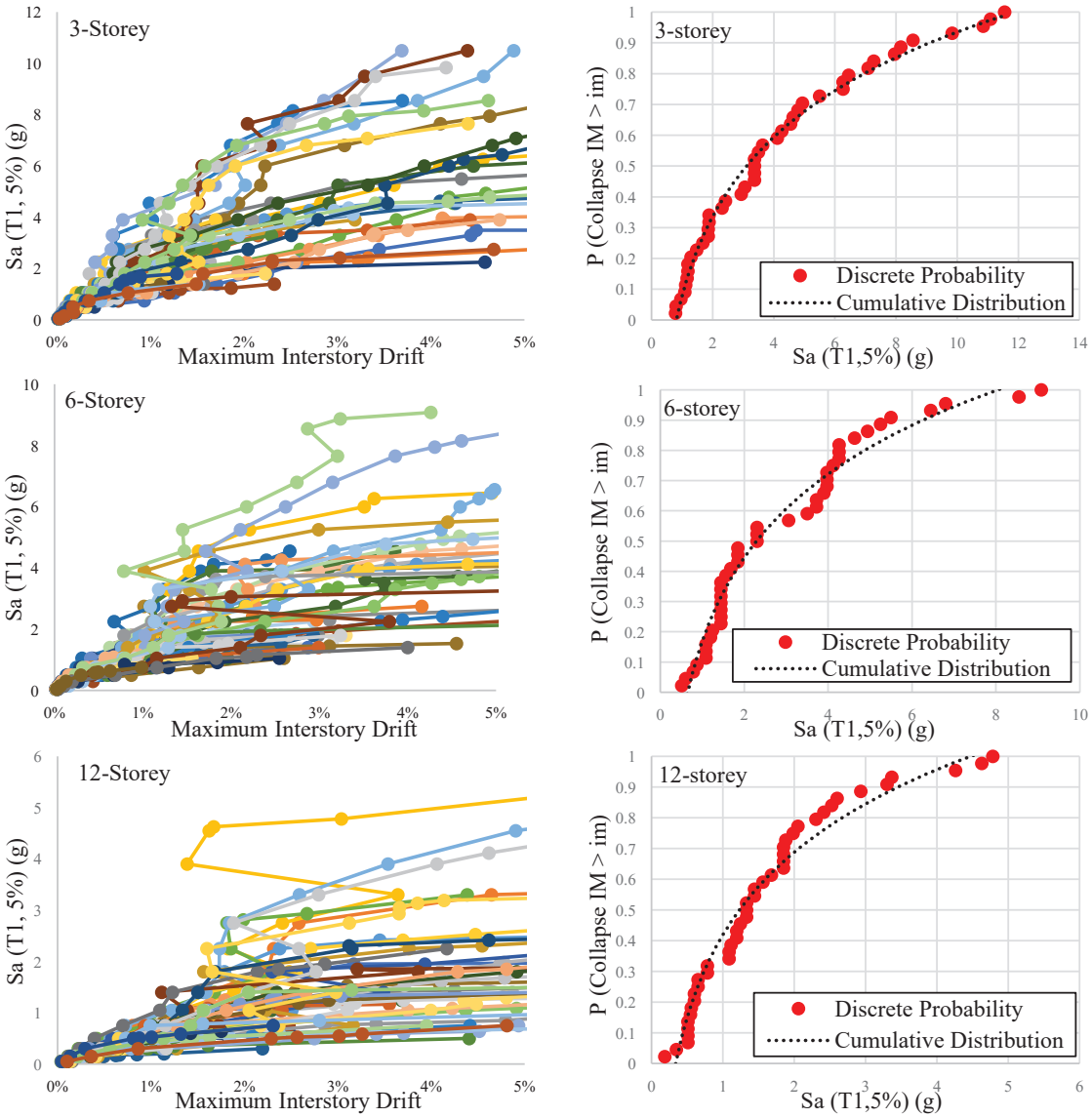

Figure 5. IDA results and collapse fragility curves.

The Record-to-Record (RTR) uncertainty refers to the variability in the response of a single archetype to different ground motion records. This variability arises from two main factors, namely differences in the frequency content and dynamic characteristics of the ground motions, and variability in hazard characterization as reflected in the Far-Field ground motion record set. A value of $\beta_{RTR} = 0.40$ is commonly used for structures with significant period elongation (i.e., those with period-based ductility $\mu_T \geq 3$), including systems with limited ductility that exhibit significant period elongation before collapse [14].

The Design Requirements (DR) uncertainty refers to the completeness and robustness of the design procedures, and the safeguards they provide against unexpected failure modes. In this study, the design standards and guidelines provided in CSA O86 [2], CSA S16 [20], and NBCC [1] were followed. While these standards do not provide specific design guidelines and procedures for TBFFJs, the well-established concept of capacity-based design was used. Therefore, for the purpose of the current study, design requirements uncertainty was rated as C (fair) and the corresponding value of $\beta_{DR} = 0.35$ was assigned.

The Test Data (TD) uncertainty refers to the completeness, robustness, and the confidence in the available test results in material, component, connection, assembly, and system level. The behaviour of wood, steel, and brass at the material level has been well investigated in structural engineering. The use of friction dampers has been studied for many years at the component level. Specifically, the behaviour of FJs in steel braced frames has been explored by numerous researchers at the assembly and system levels [24–26]. Additionally, test data is available for the use of FJs with wood specimens under both monotonic and cyclic loading at the component and assembly level [12,13]. For the purpose of the current study, the test data is rated as B (good), and the corresponding value associated with the test data uncertainty is $\beta_{TD} = 0.20$.

Finally, the Modelling (MDL) uncertainty refers to how widespread the chosen archetypes are, and how effective the analysis models are at simulating representative structural collapse behaviour. In TBFFJs, the FJs are the main sources of energy dissipation while other elements are specifically designed to remain elastic. The developed analytical model used in the current study can consider both elastic behaviour of the capacity-protected connections and frame elements, as well as the non-linear friction behaviour of the FJ. Additionally, P-delta effects are considered in the current study as a potential trigger for failure. Hence, the nonlinear model development in this study was rated as B (good) and the corresponding value associated with modelling uncertainty was assumed to be $\beta_{MBL} = 0.20$.

Therefore, the total system collapse uncertainty can be determined by combining the four previously mentioned sources of uncertainty as follows:

$$\beta_{TOT} = \sqrt{\beta_{RTR}^2 + \beta_{DR}^2 + \beta_{TD}^2 + \beta_{MDL}^2} \quad (5)$$

Using the aforementioned values for each uncertainty category, a total system uncertainty of 0.602 is obtained. The acceptable adjusted collapse margin ratio (CMR) depends on total system collapse uncertainty, β_{TOT}. A 10% probability of collapse under MCE is used for assessing the performance of a group of archetypes, while 20% is applied for each individual archetype. According to FEMA P695 [14], the acceptable ACMR for a β_{TOT} of 0.602 under MCE ground motions is 2.16 for a 10% probability of collapse and 1.66 for a 20% probability. As shown in Table 1, all archetypes meet the performance criteria prescribed by FEMA P695 procedure [14]. Therefore, the initial assumption for RMC (R) of 5 and OSF (Ω) of 1.23 is satisfying. According to FEMA P695 procedure, the OSF is conservatively rounded up to the nearest 0.5, leading to an OSF of 1.5.

Table 1: Summary of Results Obtained from Pushover and IDA Analyses for all Archetypes

Arch.	Pushover results						IDA results			Performance evaluation		
	Δ_y (mm)	Δ_u (mm)	μ	$\frac{V_d}{W}$	$\frac{V_{max}}{W}$	Ω	S_{MT} (g)	S_{CT} (g)	CMR	SSF	ACMR	PASS / Fail
3	35	450	12.99	0.2	0.265	1.33	1.5	3.367	2.244	1.33	2.985	PASS
6	159	900	5.64	0.2	0.209	1.05	1.5	2.300	1.533	1.29	1.977	PASS
12	322	1200	3.73	0.12	0.156	1.30	0.9	1.331	1.479	1.29	1.913	PASS
					Ave.	1.224				Ave.	2.292	PASS

https://doi.org/10.52202/080513-0546

5 - CONCLUSIONS

In this study, a nonlinear macro-model and modelling approach was developed and used to assess the structural performance of TBFFJs and appropriate seismic response modification and ductility-related coefficients. Using the FEMA P695 procedure, nonlinear pushover analysis and IDA were conducted using 44 ground motion records on three multi-storey (3-, 6-, and 12-storey) archetypes. The following conclusions can be drawn:

- The modelling approach adopted in this study showed good agreement between the numerical model using the developed hysteresis model and published experimental test conducted on TBFFJ under cyclic loading. Slip force, loading branch and unloading branch slopes, as well as chip points in the hysteretic behaviour of a FJ connected to a wood specimen under an axial cyclic loading were captured precisely by the developed numerical model.

- All archetypes studied herein showed ductile and stable behaviour and provided reliable safety margin against collapse. CMR and ACMR values were calculated for each archetype using the results of IDA and were compared with allowable ACMR value presented in FEMA P695. The outcome from the analysis shows a robust structural performance for all archetypes when subjected to strong ground motion.

- Satisfactory results were obtained for all designed TBFFJs during performance evaluation, which was conducted based on FEMA P695 methodology. Thus, based on the results and experimentally observed variation of FJ (reported in the literature), RMC (R) of 5 and OSF of (Ω) of 1.5 can be used to design TBFFJs.

6 - REFERENCES

[1] NRC, *National Building Code of Canada*. Ottawa, , ON, Canada: National Research Council of Canada, 2020.

[2] CSA, *Engineering Design in Wood*. Mississauga, ON, Canada: Canadian Standards Association, 2024.

[3] C. Zhiyong and P. Marjan, “Seismic Response of Braced Heavy Timber Frames with Riveted Connections,” *J. Perform. Constr. Facil.*, vol. 35, no. 5, p. 4021051, Oct. 2021.

[4] Z. Chen and M. Popovski, “Connection and System Ductility Relationship for Braced Timber Frames,” *J. Struct. Eng.*, vol. 146, no. 12, 2020.

[5] Z. Baird, J. Woods, C. Viau, and G. Doudak, “Cyclic Behavior of Bolted Glued-Laminated Timber Brace Connections with Slotted-In Steel Plates,” *J. Struct. Eng.*, vol. 150, no. 7, p. 4024068, Jul. 2024.

[6] Z. Baird, J. Woods, C. Viau, and G. Doudak, “Design considerations of braced frame bolted glulam timber connections with internal steel plates,” in *Proc., Canadian Conf.—Pacific Conf. on Earthquake Engineering*, 2023.

[7] Z. Baird, J. Woods, C. Viau, and G. Doudak, “Seismic Performance of Bolted Glulam Timber Brace Connections With Internal Steel Plates,” in *13th World Conference on Timber Engineering, WCTE 2023*, 2023, vol. 2, pp. 1176–1182.

[8] M. Popovski, E. Karacabeyli, and H. G. L. Prion, “Dynamic response of braced timber frames,” pp. 155–160, 1999.

[9] S. Mohamad Mahdi Yousef-beik, H. Bagheri, S. Veismoradi, P. Zarnani, A. Hashemi, and P. Quenneville, “Seismic performance improvement of conventional timber brace using re-centring friction connection,” *Structures*, vol. 26, pp. 958–968, 2020.

[10] M. Colton, P. C. P., B. Hans-Erik, and R. Douglas, “Development of Timber Buckling Restrained Brace for Mass Timber-Braced Frames,” *J. Struct. Eng.*, vol. 147, no. 5, p. 4021050, May 2021.

[11] C. F. Gilbert and J. Erochko, “Development and testing of hybrid timber-steel braced frames,” *Eng. Struct.*, vol. 198, p. 109495, 2019.

[12] D. Fitzgerald, A. Sinha, T. H. Miller, and J. A. Nairn, “Axial slip-friction connections for cross-laminated timber,” *Eng. Struct.*, vol. 228, p. 111478, 2021.

[13] A. Tjahyadi, “Slotted-Bolted Friction Damper as a Seismic Energy Dissipator in a Braced Timber Frame,” pp. 1–217, 2002.

[14] FEMA P-695, *Quantification of Building*

Seismic Performance Factors: Component Equivalency Methodology, no. June. Washington, DC: Federal Emergency Management Agency, 2011.

[15] G. W. Rodgers, J. G. Chase, R. Causse, J. Chanchi, and G. A. MacRae, "Performance and degradation of sliding steel friction connections: Impact of velocity, corrosion coating and shim material," *Eng. Struct.*, vol. 141, pp. 292–302, 2017.

[16] G. W. Rodgers, J. G. Chase, R. Causse, J. Chanchi, and G. A. MacRae, "Performance and degradation of sliding steel friction connections: Impact of velocity, corrosion coating and shim material," *Eng. Struct.*, vol. 141, pp. 292–302, 2017.

[17] J. C. Golondrino, G. A. MacRae, J. G. Chase, and G. W. Rodgers, "Behaviour of Asymmetrical Friction Connections using different shim materials," *2012 NZSEE Conf.*, no. 100, pp. 1–7, 2012.

[18] J. P. Davim, "Experimental study of the tribological behaviour of the brass/steel pair," *J. Mater. Process. Technol.*, vol. 100, no. 1, pp. 273–277, 2000.

[19] D. Fitzgerald, "Cross-Laminated Timber Shear Walls with Toe-Screwed and Slip-Friction Connections," Oregon State University, Corvallis, OR, USA, 2019.

[20] CSA, *Design of Steel Structures*. Toronto, ON, Canada: Canadian Standards Association, 2024.

[21] European Committee for Standardization, *Eurocode 5: Design of Timber Structures – Part 1-1: General – Common Rules and Rules for Buildings*. Brussels, Belgium: CEN, 2014.

[22] M. Popovski and Z. Chen, "Seismic Performance of Braced Timber Frames," in *Conference Proceedings*, 2024.

[23] N. Pourali, H. Khosravi, and M. Dehestani, "An investigation of P-delta effect in conventional seismic design and direct displacement-based design using elasto-plastic SDOF systems," *Bull. Earthq. Eng.*, vol. 17, no. 1, pp. 313–336, 2019.

[24] D. Vamvatsikos and C. A. Cornell, "Incremental dynamic analysis," *Earthq. Eng. Struct. Dyn.*, vol. 31, no. 3, pp. 491–514, 2002.

[25] A. S. Pall and C. Marsh, "Response of Friction Damped Braced Frames," *J. Struct. Div.*, vol. 108, no. 6, pp. 1313–1323, 1982.

[26] I. H. Mualla and B. Belev, "Performance of steel frames with a new friction damper device under earthquake excitation," *Eng. Struct.*, vol. 24, no. 3, pp. 365–371, 2002.

[27] A. Ghafouri-Nejad, M. Alirezaei, S. M. Mirhosseini, and E. Zeighami, "Parametric study on seismic response of the knee braced frame with friction damper," *Structures*, vol. 32, pp. 2073–2087, 2021.

https://doi.org/10.52202/080513-0546